Remote Sensing Reviews, 1997, Vol. 15, pp. 7–21
Reprints available directly from the publisher
Photocopying permitted by license only

© 1997 OPA (Overseas Publishers Association)
Amsterdam B.V. Published in The Netherlands
by Harwood Academic Publishers
Printed in Malaysia

Data Pre-processing: Stratospheric Aerosol Perturbing Effect on the Remote Sensing of Vegetation: Correction Method for the Composite NDVI After the Pinatubo Eruption

E. VERMOTE[a,*], N. EL SALEOUS[a], Y. J. KAUFMAN[b] and E. DUTTON[c]

[a]*Department of Geography, University of Maryland, College Park;*
[b]*NASA/GODDARD Space Flight Center/Code 913,* [c]*NOAA Climate Monitoring and Diagnostics Laboratory*

Stratospheric aerosols produced by the eruption of Mount Pinatubo in the Philippines (6 June, 1991) had a detectable effect on NOAA AVHRR data. Following the eruption, a longitudinally homogeneous dust layer was observed between 20°N and 20°S. The largest optical thickness observed for the dust layer was 0.4–0.6 at 0.5 μm. The amount of aerosols produced by Mount Pinatubo was two to three times greater than that produced by El Chichon and the Stratospheric Aerosol and Gas Experiment (SAGE) on-board the Earth Radiation Budget Experiment was not able to give quantitative estimate of aerosol optical thickness because of saturation problem.

The monthly composite Normalized Difference Vegetation Index (NDVI) (generally bounded between −0.1 and 0.6) has systematically decreased by approximately 0.15 two months after the eruption. Such atmospheric effect has never been observed on composite product and is related to the persistence and spatial extent of the aerosol layer causing the composite technique to fail. Therefore, long term monitoring of vegetation using the NDVI necessitates correction of the effect of stratospheric aerosols.

In this paper we present an operational stratospheric aerosol correction scheme adopted by the Laboratory for Terrestrial Physics, NASA/GSFC. The stratospheric aerosol distribution is assumed to be only variable with latitude. Each 9 days the latitudinal distribution of the optical thickness is computed by inverting radiances observed in AVHRR channel 1 (0.63 μm) and channel 2 (0.83 μm) over the Pacific Ocean. This radiance data set is used to check the validity of model used for inversion by checking consistency of the optical thickness deduced from each channel as well as optical thickness deduced from different scattering angles.

Using the optical thickness profile previously computed and radiative transfer code assuming lambertian boundary condition, each pixel of channel 1 and 2 are corrected prior to computation of NDVI. Comparison between corrected, not corrected, and years prior to Pinatubo eruption (1989, 1990) NDVI composite, shows the necessity and the accuracy of the operational correction scheme.

*Corresponding author: NASA/GSFC Code 923, Greenbelt, MD 20771, USA.

1. INTRODUCTION

The importance of remote sensing to provide a quantitative estimate of Earth resources and to monitor global change has been well demonstrated (Becker et al., 1988; Gatlin et al., 1983; Justice et al., 1985). The global vegetation index derived from the NOAA Advanced Very High Resolution Radiometer (AVHRR) gave the first means for scientists to study large scale natural cycles of vegetation and carbon (Tucker et al., 1985, 1986). Research to clarify the limitations of the AVHRR are in progress (Townshend & Justice, 1988, Kaufman et al., 1992; Holben et al., 1992). For example, the importance of perturbations induced by tropospheric aerosol particles has been clearly demonstrated and that subsequent reduction through compositing is being understood (Kaufman et al., 1992; Tanré et al., 1992). However, the effect of the presence of a large amount of aerosols in the stratosphere on the NDVI has never been assessed.

On June 6, 1991 Mt. Pinatubo, in the Philippines, erupted. It injected approximately two to three times more SO_2 into the stratosphere than the El Chichon eruption as estimated by SAGE (Mc Cormick & Veiga, 1992). Within a short time, the application of NDVI data for operational drought monitoring as part of the Food Early Warning System (FEWS) of the US Agency for International Development showed unusually low values of the NDVI for areas where crops were reported to be in good condition. Multidate compositing (Holben, 1986) did not appear to reduce this effect.

This aerosol effect can be clearly understood from our experience in atmospheric effects on satellite data. The stratospheric aerosol layer is composed largely of small particles (0.5 μm) located at 20 km high in the atmosphere and therefore not attenuated by water vapor or molecular scattering. A sensitivity analysis was performed using the 5S (Tanré et al., 1990) radiative transfer code which enables the simulation of the signal observed by a satellite in the solar spectrum. By considering a stratospheric aerosol model composed of small particles, the NDVI of a typical vegetation cover decreases from 0.5 to 0.4 when the optical thickness at 0.5 μm increases from 0. to 0.5. This value of optical thickness of 0.5 is in the range of expected values for stratospheric aerosols. The simulated decrease in the NDVI was comparable to that observed by the FEWS project.

In this paper we report an operational approach to correct NDVI for stratospheric aerosol effect using AVHRR data itself. A quantity proportional to the stratospheric aerosol optical thickness at 0.65 μm and 0.85 μm is derived enabling us to compute transmission and intrinsic atmospheric reflectance correction terms. These correction terms are then applied to the single channel data prior to computation of the NDVI.

2. DETERMINATION OF THE LATITUDINAL PROFILE OF STRATOSPHERIC OPTICAL DEPTH.

It has been observed by Stowe (Stowe, 1992) that a few months after a volcanic eruption, stratospheric winds produce a longitudinally homogeneous aerosol layer. In order to account for this layer, we will have to determine the latitudinal profile of these stratospheric aerosols. In this section, we will present the technique we use to determine this profile from AVHRR data. The technique used involves identifying an area over the ocean where tropospheric aerosol influence is low and therefore the stratospheric aerosol content can be derived using statistics. The area chosen is located in the Pacific Ocean and extends from 175° West to 135° West and from 60° South to 60° North. Each day, one AVHRR GAC orbit was processed, screened for clouds using CLAVR (Stowe et al., 1991), calibrated and composited with 9 other orbits by selecting the minimum value in channel 1. The composite technique enable us to better screen cloud as well as short term tropospheric aerosol event. The way of compositing orbits with no respect to the longitude of the ascending node is justified by the fact that we are looking at longitudinally homogeneous and slowly varying optical depth. It's also possible after compositing to interpret physically the signal observed because the NOAA satellite has a sun-synchronous orbit so that on a period of 9 days the only variation in geometrical condition is due to the precession of the earth.

After compositing, stratospheric optical thicknesses can be computed in both AVHRR channels by substracting the part of the signal due to Rayleigh and background tropospheric aerosol scattering and inverting the remaining radiance using a stratospheric aerosol model (King et al., 1984). The consistency of the inversion can be checked for different view angles by looking at the signal observed in both channels. Figure 1 compares for a view angle of 35° toward back scattering, the signal observed in both channels after correction of a small tropospheric background to King's model computation for a optical thickness of 0.4 at 0.55 μm for different latitudes. The same comparison is showed on Figure 2 but for a view angle of 60°. The radiative transfer computation agrees with the observation for two reasons: (a) the optical depth of 0.4 is obtained in both channel at the same latitude for the two selected angles, (b) the match between modeled and measured radiance is obtained at the same latitude for both angles. It is then possible to confidently invert the observed radiance for each composite. Figure 3 shows the optical thickness inverted from the 9 days geometrical composite before and after the stratospheric aerosol layer formation.

For additional quantitative validation we compare the deduced optical depth to the values measured at Mauna Loa observatory during the 1991–1992 period.

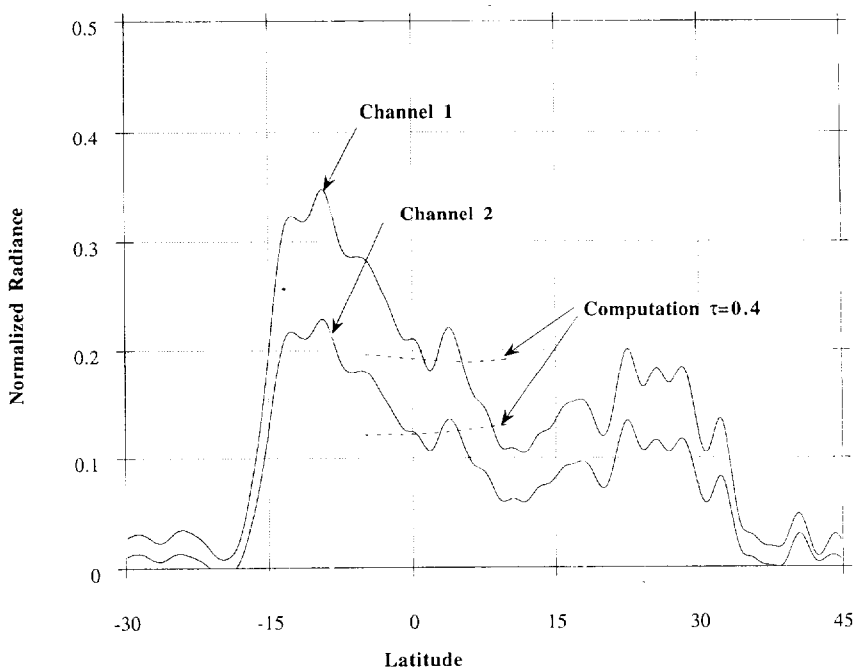

FIGURE 1 Comparison between Mt Pinatubo aerosol observed radiance and King's stratospheric aerosol model simulations for $\theta_v = 35°$

For each 9 nine days composite between 1989 and 1992, we compute an average optical depth at 0.55 μm for latitude between 19° North and 21° North. For each month, we select the minimum value observed out of 4 composites. The period 1989–1990 is used to compute the "average" tropospheric background, present in our data, but not observed at Mauna Loa because the observatory is located on a mountain of Hawaii at 3000 m altitude. The minimum monthly optical depth deduced from our process and corrected for 1989–1990 tropospheric background is compared for the 1991–1992 period to the values measured daily at Mauna Loa at 0.5 μm (Fig. 4). Before July, stratospheric aerosol background at this latitude is around 0.02. Some variation can be seen in both data sets. The variations of Mauna Loa optical depth measurements can be due to some residudals tropospheric aerosol. The variations of AVHRR retrieved optical depth is due to an improper correction of the tropospheric aerosol or to noise in the retrieval process.

The stratospheric aerosol produced by the June 1991 Mt. Pinatubo eruption can been clearly seen in both data sets starting in July 1991, the decrease after the maximum that occurs in August 1991 is also shown by both data sets and the

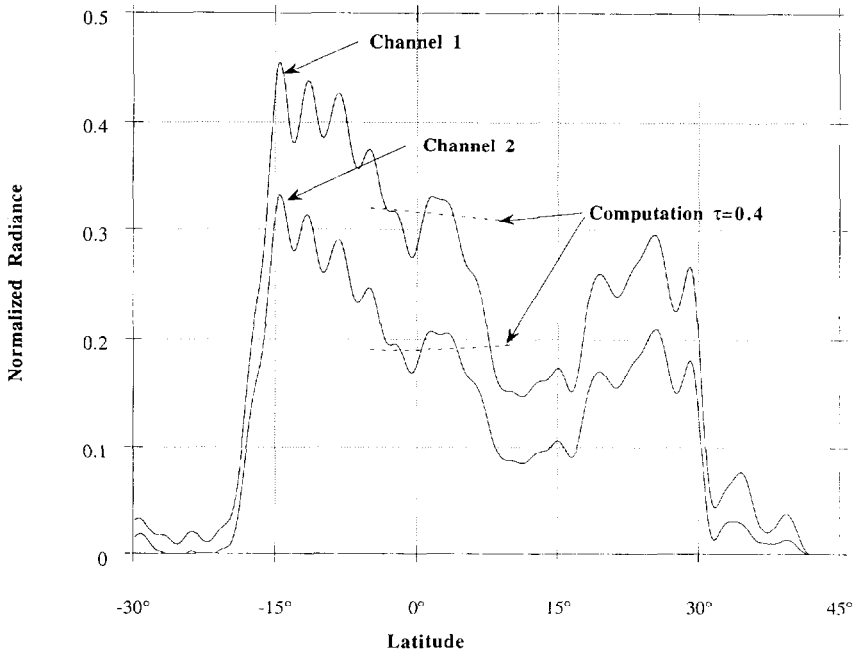

FIGURE 2 Same as figure 1 for $\theta_v = 60°$

e folding time is of the order of a year and a half. There are differences between the two that can be explained by the variability of the stratospheric aerosol thickness during the period of one month or some unfiltered tropospheric events or in homogeneity in the longitudinal distribution of the stratospheric aerosol.

Figure 5, shows the comparison between the wavelength exponent of the aerosol deduced from the two channels of AVHRR (0.63 μm and 0.87 μm) and from the three wavelengths of the Mauna Loa data set (0.38 μm, 0.50 μm and 0.78 μm). Both data sets shows a change in the wavelength exponent suggesting an evolution of the size distribution of the stratospheric aerosol to bigger particles. The King's model gives an exponent of −0.75 that can be observed in July and August 1991.

The data of Mauna Loa are very useful for comparison purposes but cannot give the spatial distribution of the stratospheric aerosol. As shown by figure 6, the largest concentration were located in the 10° South to 10° North zone and the maximum value is double of the largest value observed at Mauna Loa.

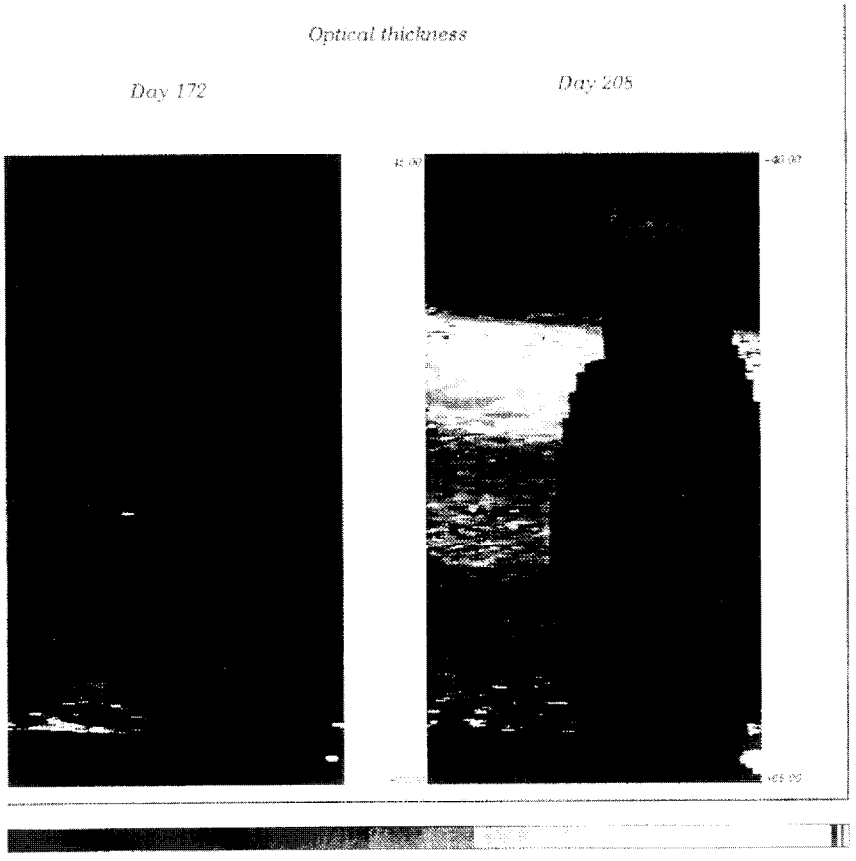

FIGURE 3 "Geometric" composite of the optical thickness in channel 1 of AVHRR before and after the stratospheric aerosol layer formation. (See Colour Plate I at the back of the journal).

3. CORRECTION EQUATION FOR NDVI 30 DAY COMPOSITE

The AVHRR data used in this study was Global Area Coverage (GAC) data from the NOAA-11 satellite. The NDVI is computed from AVHRR visible (0.63 μm) and near infrared (0.87 μm) preflight calibrated digital counts, DC_1 and DC_2 according to Eq. (1)

$$NDVI = \frac{DC_2 - DC_1}{DC_2 + DC_1} \tag{1}$$

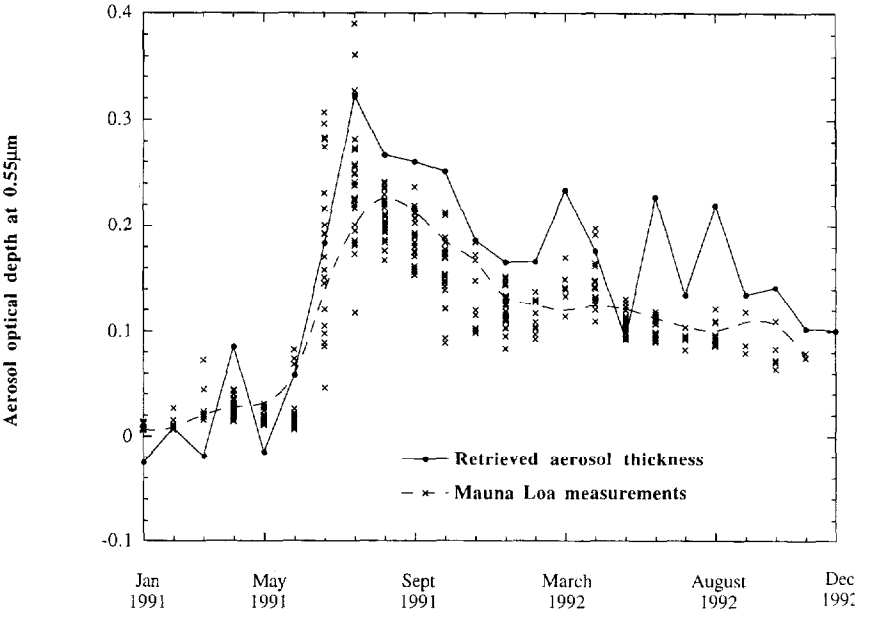

FIGURE 4 Comparison between retrieved "stratospheric" optical thickness and measurements taken at Manua Loa observatory

If we want to correct only for the perturbation caused by the stratospheric aerosol, in order to be able to compare these data with historical data sets that had no atmospheric correction, we can approximate the stratospheric aerosol effect on each channel, by considering a lambertian ground + troposphere system, by:

$$DC^{perturbed} = DC^{stratosphere}(\phi) + T(\mu_s)T(\mu_v)DC^{corrected} \quad (2)$$

where μ_s, μ_v and ϕ are the cosine of the solar zenith angle, the cosine of the view angle and the azimuthal difference between the Sun and the sensor respectively

$DC^{stratosphere}$ is the stratospheric aerosol contribution.

$T(\mu)$ is the transmission (upward for μ_v, downward for μ_s) of the stratospheric aerosol layer.

The stratospheric path radiance, $DC^{stratosphere}$, is computed using King stratospheric aerosol model (King et al., 1984). For 17 view angles, 22 sun zenith angles, 81 relative azimuth angles and 10 optical depths (ranging from 0.05 to

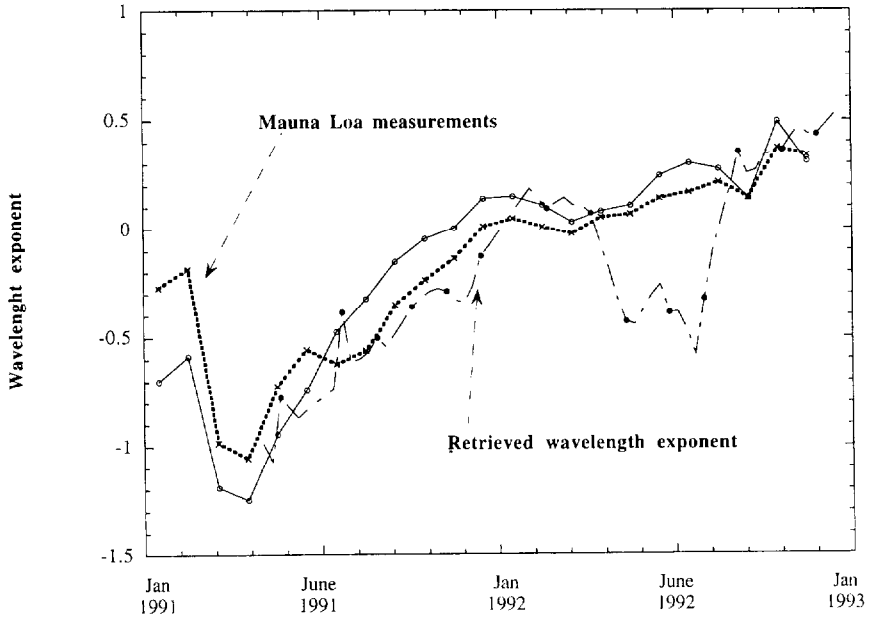

FIGURE 5 Same as figure 4 for the wavelength exponent

0.5) a table that gives the path radiance in both channels was computed a computer code using the Successive Order of Scattering, SOS, method (Deuzé et al., 1989).

The transmission has been fitted in both channels using the following approximate formula:

$$\mathbf{T}(\mu) = \mathbf{e}^{-(a\tau\mu^{b})} \tag{3}$$

The accuracy of equation 3 is sufficient for the NDVI correction scheme as shown by Figure 7a–b. For angles ranging from nadir to 70° and optical depth ranging from 0.05 to 0.5 the approximation was compared to the "exact" computation performed using the SOS method.

4. ERROR BUDGET

The error in the NDVI correction is different for different cover types. We selected bare soil and evergreen forest as the two extreme cases. The solar zenith angle is fixed to 45° as an average of the variation between summer and winter and the viewing angle is set to nadir because the compositing process trends to

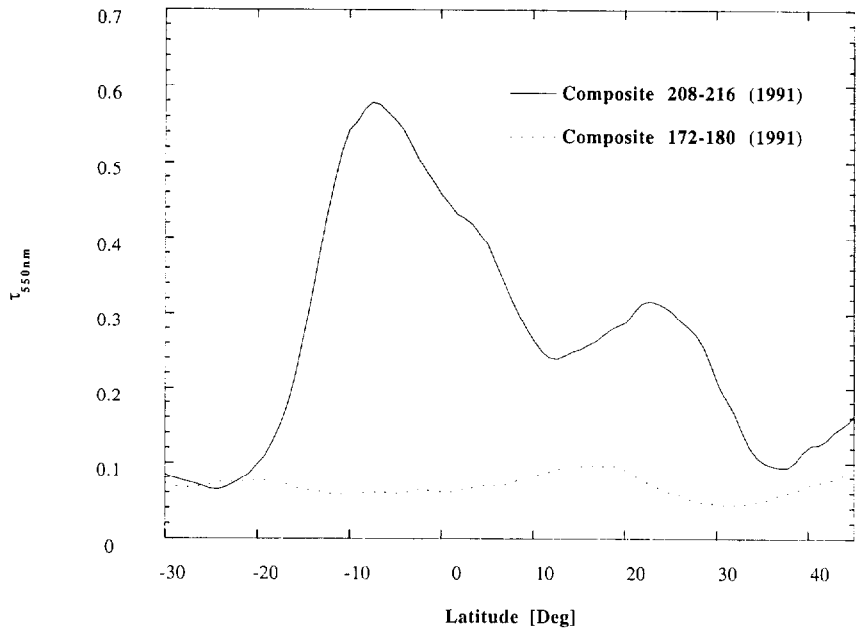

FIGURE 6 Latitudinal "stratospheric" profile observed after Mt. Pinatubo eruption

reject off nadir pixels. The approximation of Eq. (2) to correct the stratospheric effect is unavoidable, to properly correct the data one will have to take into account the non-lambertianity of both atmosphere and surface. For the surface, the directional properties are not available so far. The error made on NDVI can be approximated by the study of Lee and Kaufman (1986), from their paper they pointed out error up to 0.04 for turbid atmosphere, this refer to the net error on NDVI due to non-lambertianity. In our case where we are only interested in evaluating the NDVI at the top of the atmosphere, the error to be considered should be lower, an error of 0.02 NDVI unit in case of high optical depth (0.6) and 0.01 for lower optical depth (0.3) is considered.

Two other sources have to be considered, the error due to incorrect optical depth and the error done by using an improper aerosol model. Table I gives for the two surfaces considered, the NDVI at the top of the atmosphere for a 0.05 tropospheric aerosol optical depth and a tropical atmospheric profile, it gives also the effect on NDVI of a high and average (0.6, 0.3) stratospheric aerosol optical depth. Table II gives the error associated with an uncertainty of ± 0.05 optical depth. The error due to change in size distribution is also reported for an optical depth of 0.3, by varying the wavelength exponent from the King et al model values to 0. From this table, the rms error of the correction scheme can be

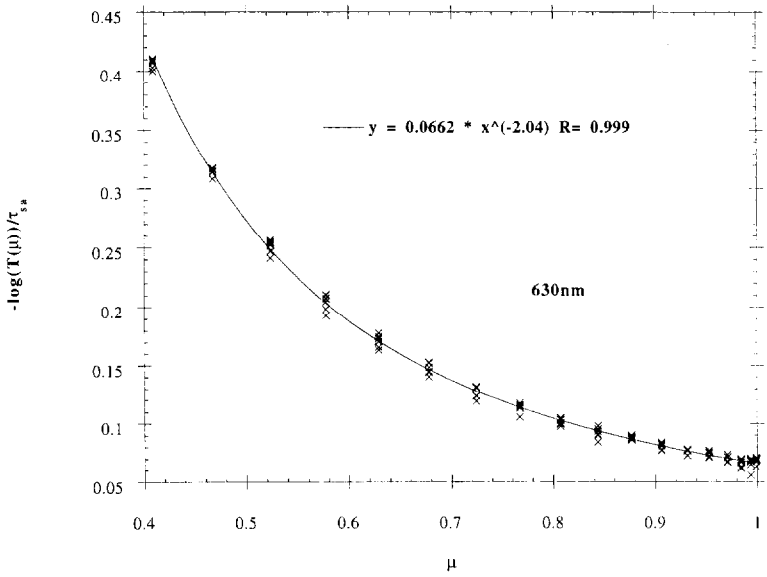

FIGURE 7a Comparison between "exact" computation and Eq. 3 approximation for transmission function at 630 nm

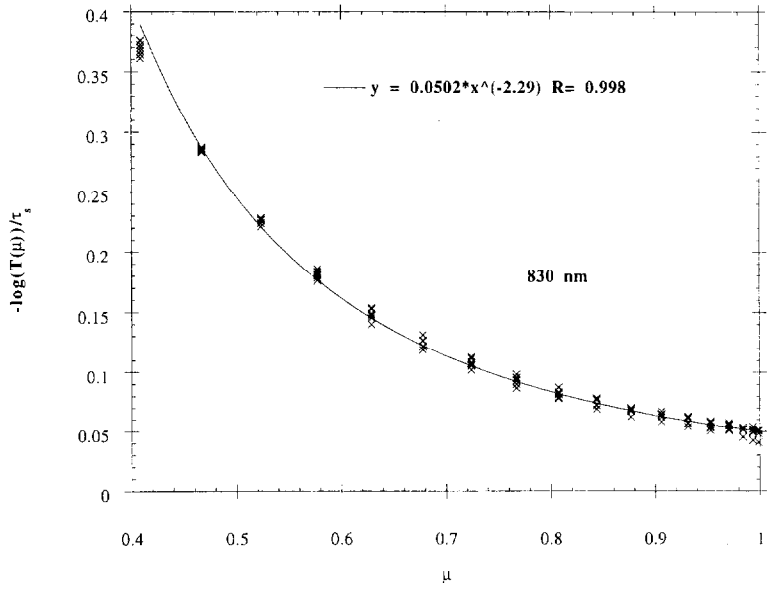

FIGURE 7b Same as figure 7a at 830 nm

TABLE II Error budget for Mt. Pinatubo aerosol correction

Case	*Error on NDVI* $\tau_s = 0.6$	*Error on NDVI* $\tau_s = 0.3$
Non Lambertianity	±0.02	±0.01
Bare Soil $\Delta\tau_s = \pm 0.05$	±0.001	±0.0015
Evergreen forest $\Delta\tau_s = \pm 0.05$	±0.008	±0.009
Bare Soil Wav. Exp. = 0.	-	−0.041
Evergreen forest Wav. Exp. = 0.	-	0.550

computed, it is of the order of 0.01 for optical depth of 0.3 and double for optical depth of 0.6. The overall accuracy of the correction is then to correct 80% of the effect.

5. VALIDATION OF NDVI CORRECTION

A preliminary validation has been undertaken, comparing corrected NDVI with the uncorrected for a sample area of 20 by 20 degrees over east Africa centered on the equator. A nine days composite of the NDVI has been computed for 1989–1992 before and after the stratospheric aerosol layer formation. Figure 8 shows the histogram of NDVI before the effect is detectable. The distribution of NDVI for 1991 is comparable to the one observed in 1989/1990 especially in the higher range of NDVI [0.4–0.6]. Figure 9 gives the same distribution for a 9 days composite at the beginning of August. The uncorrected data of 1991 are lower by 0.10–0.15 NDVI units than the 1989/1990 values, the corrected values are falling exactly in the range of the previously observed values. The same comparison is conducted in 1992, Figure 10, in that case the effect of stratospheric aerosol is lower, 0.05 NDVI unit, and the corrected values fit better the previous year for higher NDVI. The agreement between corrected and previous year NDVI is not so good in the intermediate range of NDVI values [0.15–0.4].

TABLE I Simulated NDVI

Case	*NDVI*	*Simulated NDVI (before Pinatubo) top of the atmosphere*	*Simulated NDVI (after Pinatubo) T.O.A.* $\tau_S = 0.6$	*Simulated NDVI (after Pinatubo) T.O.A.* $\tau_S = 0.3$
Bare Soil $\rho_1 = 0.19$, $\rho_2 = 0.22$	0.073	−0.043	−0.051	−0.048
Evergreen forest $\rho_1 = 0.02$, $\rho_2 = 0.36$	0.846	0.600	0.493	0.547

This is probably due to a change in NDVI values. As shown by Figure 8, only the higher range and the lower range of NDVI is expected to be stable over the year because it covers area where man activities is less important (Desert, Evergreen Forest).

6. CONCLUSION

Comprehensive validation of the correction is problematic in that it requires both an independent assessment of stratospheric and tropospheric aerosols as well as vegetation state. We are highly dependent on the quality of the aerosol retrieval particularly with respect to the spatial and temporal coverage. However, we are confident in the radiative transfer computation that have been made.

The effects of the Pinatubo eruption on the NDVI will need correction until the magnitude of the effect becomes part of the background atmospheric noise in the NDVI signal. Given the rate of decay we estimate this to be approximately towards the begin of 1993. Clearly in the long term, the research community

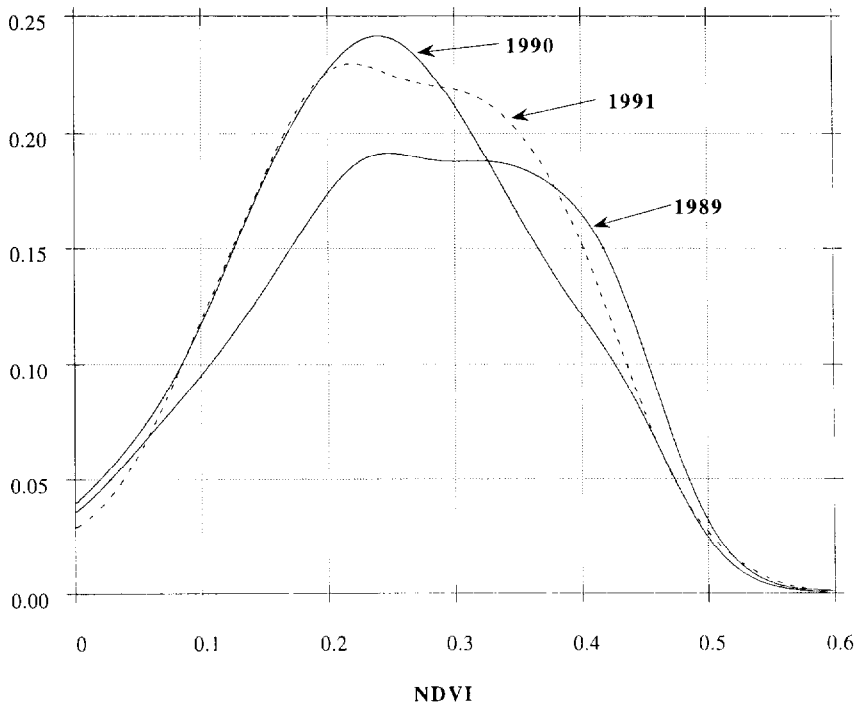

FIGURE 8 Histogram of NDVI over Africa (10°S to 10°N) before Mt. Pinatubo aerosol effect.

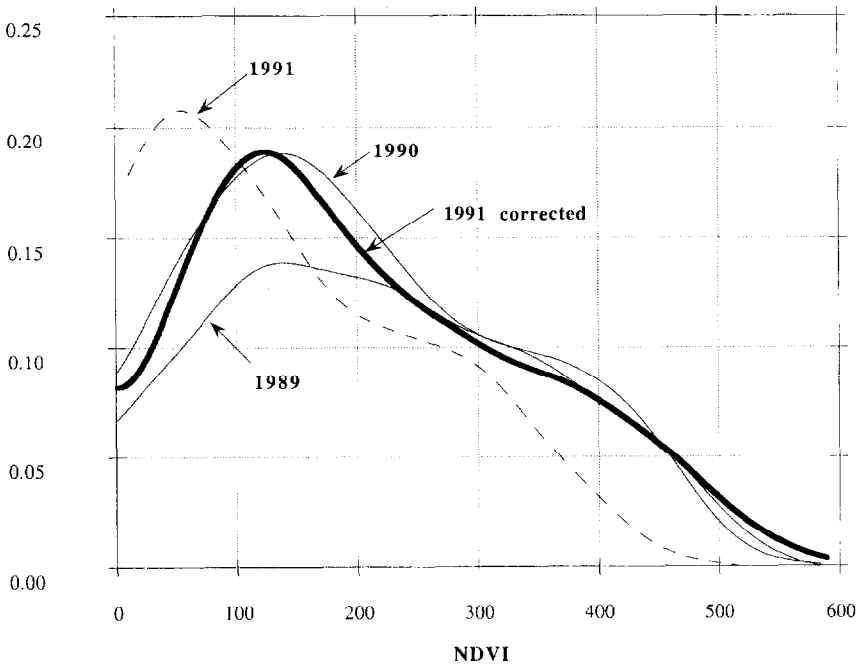

FIGURE 9 Comparison of histogram of corrected, uncorrected and previous year NDVI for 1991 after the eruption.

must move towards an operational and comprehensive atmospheric correction including all aerosol effects (Vermote et al., 1993). Until this has been accomplished, we are obliged to apply corrections as presented here. The present study must be seen in this context and has raised several issues relevant to the operational atmospheric correction planned for the EOS generation sensors.

The objective of this study was to develop a quick and effective correction procedure that could be applied operationally to the AVHRR data for the generation of NDVI. Within the limits of our validation exercise this has been achieved. However, a complete characterization of stratospheric aerosols is an area for future research and is beyond the scope of this present activity. Two "corrected" global vegetation index data set are or will be available soon, the 1° × 1° FAZIR data set (Los et al., 1994) produced using GIMMS Pinatubo corrected data set, and the 8 km NOAA GVI (Vermote & Kaufman, 1993).

Acknowledgements

The authors wish to thank Brent Holben and Chris Justice of the GIMMS group at NASA/GSFC as well as Graham Farmer from the FEWS project for their

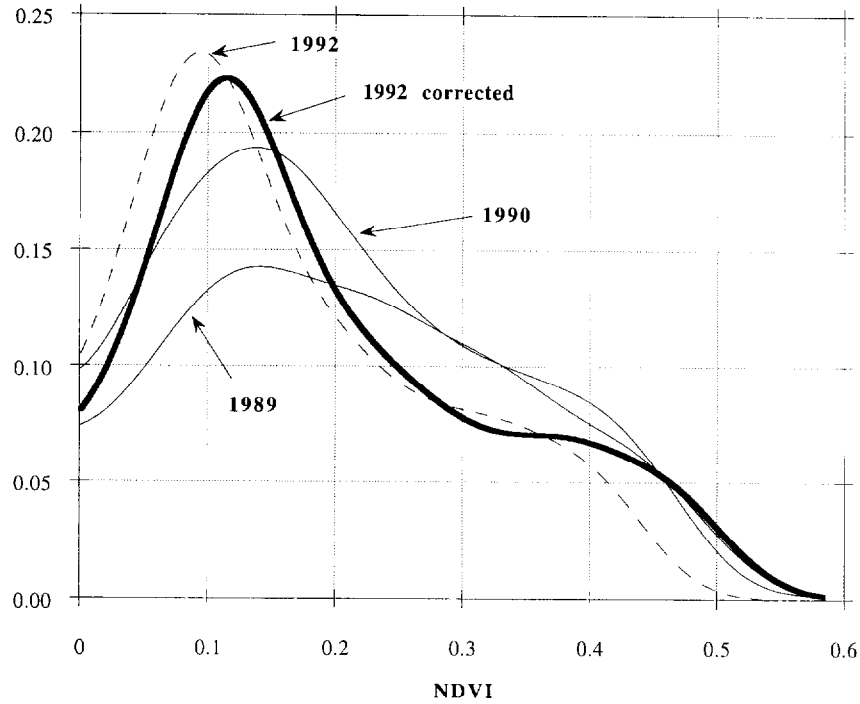

FIGURE 10 Same as figure 9 but for 1992.

useful comments on this research and to Jim Tucker for providing the AVHRR data.

References

Becker, F., Bolle, H. J. and Rowntree, P. R., 1988. *The International Satellite Land-Surface Climatology Project (ISLSCP)* (Berlin: United Nations Environmental Programme ISLSCP Secretariat).

Deuzé, J. L., Herman, M. and Santer, R., 1989. Fourier series expansion of the transfer equation in the atmosphere-ocean system. *Journal of Quantitative Spectroscopy and Radiative Transfer*, **41**, 6, 483–494.

Gatlin, J. A., Sullivan, B. and Tucker, C. J., 1983. Monitoring global vegetation using NOAA AVHRR data. *Proc. of the IGAARS Symp., 1983, San Francisco California*, I IEEE), pp. 71.

Holben, B. N., 1986. Characteristics of maximum-value composite images for temporal AVHRR data. *Int. J. Remote Sens.*, **7**: 1435–1445.

Holben, B. N., Vermote, E., Kaufman, Y. J., Tanré, D. and Kalb, V., 1992. Aerosol Retrieval over Land from AVHRR data-Application for Atmospheric Correction. *IEEE Trans. Geosci. Remote Sens.*, **30**: 212–222.

Justice, C. O., Townshend, J. R. G., Holben, B. N. and Tucker, C. J., 1985. Analysis of the phenology of global vegetation using meteorological satellite data. *Int. J. Remote Sens.*, **6**: 1271–1318.

Kaufman, Y. J., Tanré, D., Holben, B. N., Markham, B. and Gitelson, A., 1992. Atmospheric effects on the NDVI—Strategies for its removal. *Proc. IGARSS*, 2 IEEE), pp. 1238–1241.

King, M., D, Harshvardhan and Arking, A., 1984. A model of the radiative properties of the El Chichon Stratospheric Aerosol layer. *Jo. Climate Appl. Meteor.*, **23**, 1121–1137.

McCormick, M., P and Veiga, R., E, 1992. SAGE II Measurements of early Pinatubo aerosols. *Geophys. Res. letters*, **19**: 155–158.

Lee, T. Y. and Kaufman, Y. J., 1986. Non-Lambertian effects on remote sensing of surface reflectance and vegetation index. *IEEE Trans. Geosci. Remote Sens.*, GE-**24**: 699–708.

Los, S. O., Justice, C. O. and Tucker, C. J., 1994. A Global 1° × 1° NDVI data set for climate studies derived from the GIMMS continental NDVI, *Int. J. Remote Sens.*, (In press)

Stowe, L. L., McClain, E. P., Carey, R., Pellegrino, P., Gutman, G. G., Davis, P., Long, C. and Hart, S., 1991. Global Distribution of Cloud Cover derived from NOAA/AVHRR operational Satellite Data. *Adv. in Space Research/COSPAR*, 11 COSPAR), pp. 51–54.

Stowe, L. L., Carey, R. M. and Pellegrino, P. P., 1992. Monitoring the Mt. Pinatubo aerosol layer with NOAA/11 AVHRR data. *Geophys. Res. Letter*, **19**: 159–162.

Tanré, D., Deroo, C., Duhaut, P., Herman, M., Morcette, J. J., Perbos, J. and Deschamps, P. Y., 1990. Description of a computer code to simulate the satellite signal in the solar spectrum: 5S code". *Int. J. Remote Sens.*, **11**: 659–668.

Tanré, D., Holben, B. N. and Kaufman, Y. J., 1992. Atmospheric Correction algorithm for NOAA-AVHRR Products: Theory and Application. *IEEE Trans. Geosci. Remote Sens.*, **30**: 231–248.

Townshend, J. R. G. and Justice, C. O., 1988. Selecting the spatial resolution of satellite sensors required for global monitoring of land transformations. *Int. J. Remote Sens.*, **9**: 187–236.

Tucker, C. J., Vanpraet, C. L., Sharman, M. J. and Van Ittersum, G., 1985. Satellite remote sensing of total herbaceous biomass production in the Senegalese Sahel: 1980–1984. *Remote Sens. Environ.*, **17**: 233–249.

Tucker, C. J., Fung, I. Y., Keeling, C. D. and Gammon, R. H., 1986. The Relationship of Global Green Leaf Biomass to Atmospheric CO_2 Concentrations. *Nature*, **319**: 159–199.

Vermote E., Remer L., Kaufman, Y. J. and Justice C. O., 1993. Atmospheric correction of MODIS visible and near infrared channels, Algorithm Technical Background Document, draft version 0

Vermote E. and Kaufman, Y. J., 1993. Rayleigh, ozone and stratospheric aerosol effect correction for NOAA-GVI dataset, Report.

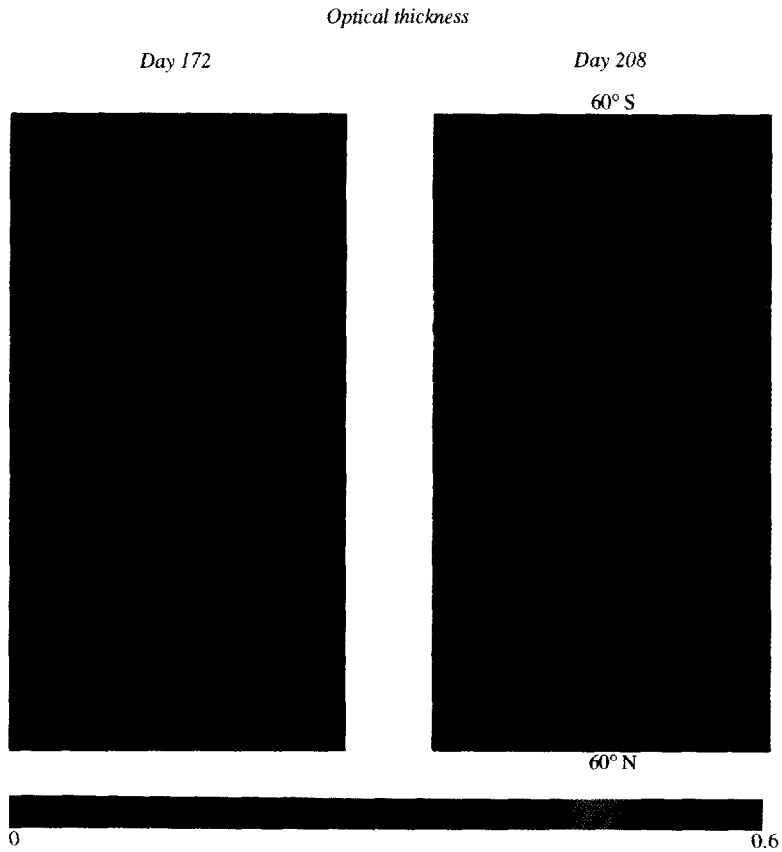

COLOUR PLATE I

FIGURE 3 "Geometric" composite of the optical thickness in channel 1 of AVHRR before and after the stratospheric aerosol layer formation. (See page 12).